

## Mimicing surface phonon polaritons in microwave band based on ionic-type phononic crystal

Xi-kui Hu, Yang Ming, Xue-jin Zhang, Yan-qing Lu, and Yong-yuan Zhu

Citation: *Appl. Phys. Lett.* **101**, 151109 (2012); doi: 10.1063/1.4758467

View online: <http://dx.doi.org/10.1063/1.4758467>

View Table of Contents: <http://apl.aip.org/resource/1/APPLAB/v101/i15>

Published by the [American Institute of Physics](#).

---

### Related Articles

Controlled spatial switching and routing of surface plasmons in designed single-crystalline gold nanostructures  
*Appl. Phys. Lett.* **101**, 141114 (2012)

Surface plasmon amplification characteristics of an active three-layer nanoshell-based spaser  
*J. Appl. Phys.* **112**, 074309 (2012)

Plasmonic concentrator of magnetic field of light  
*J. Appl. Phys.* **112**, 074304 (2012)

Strong coupling effects between a meta-atom and MIM nanocavity  
*AIP Advances* **2**, 032186 (2012)

Surface plasmon coupling efficiency from nanoslit apertures to metal-insulator-metal waveguides  
*Appl. Phys. Lett.* **101**, 121112 (2012)

---

### Additional information on *Appl. Phys. Lett.*

Journal Homepage: <http://apl.aip.org/>

Journal Information: [http://apl.aip.org/about/about\\_the\\_journal](http://apl.aip.org/about/about_the_journal)

Top downloads: [http://apl.aip.org/features/most\\_downloaded](http://apl.aip.org/features/most_downloaded)

Information for Authors: <http://apl.aip.org/authors>

## ADVERTISEMENT



**Goodfellow**  
metals • ceramics • polymers • composites  
70,000 products  
450 different materials  
**small quantities fast**

[www.goodfellowusa.com](http://www.goodfellowusa.com)

# Mimicing surface phonon polaritons in microwave band based on ionic-type phononic crystal

Xi-kui Hu, Yang Ming, Xue-jin Zhang,<sup>a)</sup> Yan-qing Lu,<sup>a)</sup> and Yong-yuan Zhu  
*National Laboratory of Solid State Microstructures, Nanjing University, Nanjing 210093,  
 People's Republic of China*

(Received 1 April 2012; accepted 27 September 2012; published online 9 October 2012)

We propose an approach to scale the frequency of surface phonon polariton to megahertz-gigahertz region via an artificial microstructure, ionic-type phononic crystal (ITPC). The period of ITPC can be intentionally controlled on all relevant length scales, which allows the creation of surface phonon polariton with almost arbitrary dispersion in frequency and space. A field of surface phonon polariton optics in microwave band is expected with similar optical properties to those of ionic crystals in infrared. © 2012 American Institute of Physics. [<http://dx.doi.org/10.1063/1.4758467>]

Surface polariton (SP) is collective excitation when electromagnetic (EM) surface waves propagate along the surface of materials that enable confinement and control of EM energy at subwavelength scales.<sup>1–6</sup> So far, researches of SP have even extent to a single atomic layer.<sup>7</sup> Surface phonon polariton (SPhP)<sup>8–10</sup> reveals the coupling between EM field and lattice vibration around the surface of ionic crystals. Although it attracts less attention than surface plasmon polariton (SPP), there are still many useful prospects in surface enhanced infrared (IR) absorption and transmission,<sup>11</sup> high-density IR data storage,<sup>12</sup> coherent thermal emission,<sup>13</sup> subwavelength scale phononic photonics,<sup>14</sup> and negative index metamaterials.<sup>15</sup> However, due to the material's natural characteristics, SPhP is normally excited in a narrow and fixed frequency range in infrared. Subwavelength microwave phenomena are hard to be observed. It would be much desired to effectively adjust and control the excitation frequency of SPhPs just like the mimicking low frequency SPPs.<sup>16,17</sup>

Generally, ionic crystals are constituted of dipoles that determine the dielectric response.<sup>18</sup> When EM waves propagate along the surface of an ionic crystal, the dipoles are polarized to form the charge distribution. Therefore the SPhP is excited in negative permittivity region to satisfy the EM boundary condition. As the dipoles are usually composed of positive and negative ions, they are in the lattice scales. Therefore, the excited SPhPs are typically in infrared. If the dipole size is enlarged, the corresponding wavelength would be larger with lower frequency. On the other hand, ionic-type phononic crystal (ITPC), scilicet piezoelectric superlattice, has been proposed to be a counterpart of ionic crystal in microwave band.<sup>19</sup> It has been realized for arbitrary polarized and structured piezoelectric superlattice,<sup>20</sup> and its phonon polariton dispersion has been deeply studied.<sup>21</sup>

ITPC is a kind of artificial media with ferroelectric domain or piezoelectric coefficient being modulated, in which the interaction between the superlattice vibration and EM wave may be established. And it exactly provides size

increased “dipoles.” In comparison with ionic crystal, ITPC has similar but tunable dielectric characteristics. The corresponding frequency with abnormal negative permittivity moves to megahertz-gigahertz band. Therefore, in this letter, we propose to realize ITPC based SPhP mode in microwave band. Similar optical properties to those of ionic crystals in infrared can be expected.

Typically, we can explain the dielectric properties of ionic crystals by one-dimensional (1D) diatomic chain structure with positive and negative ions. In the simplest case, when an EM field is supplied, positive and negative ions have relative displacement  $u_+ - u_-$  due to lattice vibrations, and then the dielectric response of EM field can be described by Huang's equations<sup>18</sup>

$$\begin{cases} \ddot{W} = b_{11}W + b_{12}E \\ P = b_{21}W + b_{22}E \end{cases}, \quad (1)$$

where  $W = \rho^{1/2}(u_+ - u_-)$  indicates crystal vibrations,  $\rho$  is equivalent density,  $E$  is external electric field intensity, and  $P$  is crystal polarization. In an ITPC,<sup>19–21</sup> as a scale enlarged ionic crystal, the similar properties have been proven. As shown in Fig. 1, the typical structure is composed of two piezoelectric domains with a periodic superlattice structure. Compared with lattice vibrations of ionic crystals, the relative motion is caused by the piezoelectric effect.

In piezoelectric materials, set the strain  $S$  and electric field intensity  $E$  as the independent variables, the fundamental equations are piezoelectric equations<sup>22</sup>

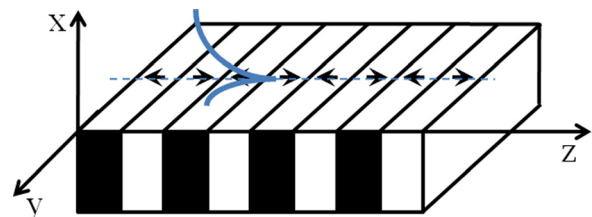


FIG. 1. Schematic of an ITPC consisting of two kinds of ferroelectric media. The arrows represent the orientation of the spontaneous polarization. The blue arc represents that there is SPhP mode at the interface between ITPC and vacuum.

<sup>a)</sup>Authors to whom correspondence should be addressed. Electronic addresses: yqlu@nju.edu.cn and xuejinzh@nju.edu.cn.

$$\begin{cases} T = cS - e^T E \\ D = eS + \varepsilon E \end{cases}, \quad (2)$$

where  $T$  is stress,  $D$  is electric displacement vector,  $\varepsilon$  is the dielectric constant,  $c$  is the elastic constant, and  $e$  is the piezoelectric coefficient. As shown in Fig. 1, the simplest case in which the ITPC is composed of two domains with the same thickness and elastic properties was chosen. The two kinds of “ions” constitute “dipoles,” scilicet two piezoelectric domains, whose relative motion can be influenced by an EM field, especially that of a microwave. This process is equivalent to the polarization in ionic crystals. These two kinds of “ions” constitute dipoles, parallel to positive and negative ions in ionic crystals. The motion of domain boundaries with positive and negative charges is defined as  $S_+$  and  $S_-$ , respectively. Under the condition of long-wavelength approximation, the motion of each primitive cell can be viewed as identical. Thus, using Newton’s motion law and treating the ITPC as a 1D chain with discrete equivalent mass dots at domain boundaries, in the lossless limit, we obtain the equations of the relative motion of these mass dots

$$\begin{cases} \ddot{W} = b_{11}W + b_{12}E \\ P = b_{21}W + \varepsilon_0(\varepsilon - 1)E \end{cases}, \quad (3)$$

where  $W = \rho^{1/2}l(S_+ - S_-)/2$ , herein  $l$  is the domain thickness.

Comparing Eq. (1) with Eq. (3), we find that they have the same format, which means that the Huang’s equations and piezoelectric equations are equivalent. Therefore, parameters in Eq. (3) are acquired as  $b_{11} = -\pi^2 v^2 / l^2$ ,  $b_{12} = b_{21} = 2e / \rho^{1/2} l$ , and  $b_{22} = \varepsilon_0(\varepsilon - 1)$ . The spoof angular eigenfrequency of the transverse vibration without the coupling of external EM field is  $\omega_{TO} = (-b_{11})^{1/2}$ , and the spoof angular eigenfrequency of the longitudinal wave is  $\omega_{LO} = [-b_{11} + b_{12}^2 / (\varepsilon_0 + b_{22})]^{1/2}$ . Generally,  $\omega_{LO}$  is larger than  $\omega_{TO}$ , because the electrostatic-like field formed by longitudinal vibration increase the resilience of the oscillator. Then, the dielectric response will be got from Eq. (3)

$$\varepsilon(\omega) = \varepsilon(\infty) \frac{\omega_{LO}^2 - \omega^2}{\omega_{TO}^2 - \omega^2}. \quad (4)$$

According to the Eq. (4) above, the dielectric response of an ITPC agrees perfectly with the Lyddane-Sachs-Teller relationship in ionic crystal. That is to say the ITPC’s dielectric response is analogous to those of ionic crystal. Therefore, ITPC and ionic crystal have similar optical properties. But for an ITPC, both  $\omega_{TO}$  and  $\omega_{LO}$  can be changed by varying the domain thickness or choosing different piezoelectric media. Thus, the  $\varepsilon(\omega)$  is controllable, indicative of tunable optical properties in ITPC.

In the actual crystals, due to scattering, absorption, and other processes, the loss is inappropriate to be ignored.<sup>23</sup> Without loss of generality, by employing a damping term  $-i\gamma\dot{W}$  in the right side of Eq. (3), we get

$$\begin{cases} \ddot{W} = -i\gamma\dot{W} + b_{11}W + b_{12}E \\ P = b_{21}W + \varepsilon_0(\varepsilon - 1)E \end{cases}. \quad (5)$$

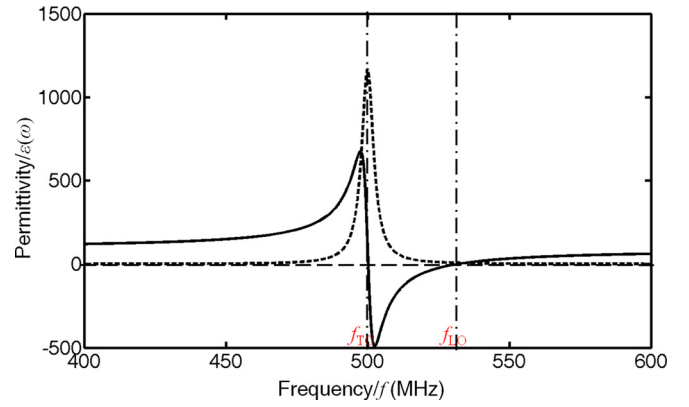


FIG. 2. The calculated dielectric response curves of an ITPC. The solid line represents the real part of  $\varepsilon(\omega)$ , and the dashed line represents the imaginary part.

The dielectric response will be modified to be

$$\varepsilon(\omega) = \varepsilon(\infty) \frac{\omega_{LO}^2 - i\gamma\omega - \omega^2}{\omega_{TO}^2 - i\gamma\omega - \omega^2}. \quad (6)$$

Figure 2 shows the dielectric dispersion curve of an ITPC based on a Z-directional modulated periodically poled LiNbO<sub>3</sub> (PPLN) with the period of 7.2  $\mu\text{m}$  by choosing a proper damping term ( $\gamma = 0.01\omega_{TO}$ ).<sup>19</sup> The dielectric spectrum in this band (400–600 MHz) shows the same curve shape as the far-infrared dielectric constant of an ionic crystal caused by lattice vibration, meaning that they have a similar origin. It is possible that the ITPC generates spoof phonons in microwave band. The dielectric response  $\varepsilon(\omega)$  are insensitive in the low or high frequencies, while they evidently change with frequencies around the transverse eigenfrequency  $f_{TO} = \omega_{TO}/2\pi = 500$  MHz, owing to the photon-phonon interaction. The real part of  $\varepsilon(\omega)$  have two zero points, one is in transverse eigenfrequency  $f_{TO}$ , and another one is in longitudinal eigenfrequency  $f_{LO} = \omega_{LO}/2\pi = 532$  MHz. From the figure,  $\varepsilon(\omega)$  is negative between  $f_{TO}$  and  $f_{LO}$ , giving the possibility to generate spoof SPhP on the surface of ITPC in this range.

We also calculate the dispersion curves of both bulk and surface polaritons as shown in Fig. 3. The black solid lines represent the real parts and black dashed lines represent the imaginary parts. However, the ITPCs bulk effect has a band gap with negative dielectric response between the frequencies  $f_{TO}$  and  $f_{LO}$ , analogy to ionic crystal in IR. Although light cannot propagate in the ITPC, SPhP-like mode can be generated on the surface of ITPC to fill in the band gap. That is because surface mode could exist with certain negative values of  $\varepsilon$ .<sup>1</sup> Just considering a simple case, this surface mode is clipped at the interface of vacuum and ITPC; here, both vacuum and ITPC are semi-infinite. SPhP can be generated only with TM mode, whose electrical field distribution can be written as

$$\begin{cases} E_{z1} = E_{z1}^0 \exp(-\alpha_1 x) \exp(i(k_{SPhPz} z - \omega t)) \\ E_{z2} = E_{z2}^0 \exp(-\alpha_2 x) \exp(i(k_{SPhPz} z - \omega t)) \end{cases}. \quad (7)$$

The symbols  $E_{z1}$  and  $E_{z2}$  represent vacuum and ITPC, respectively,  $E_z$  represents a z-directional polarized EM field,

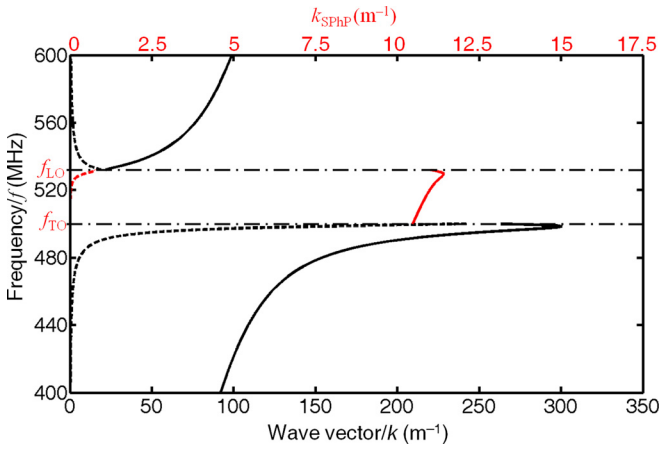


FIG. 3. Dispersion relation ( $f$ - $k$  curves) of an ITPC. Black lines represent the bulk polariton dispersion of the ITPC and red lines represent the SPhP. Solid lines represent the real parts, and dashed red lines represent the imaginary parts.

$E^0$  represent the initial EM field at the interface,  $\omega$  is the angular frequency, and  $k_0$  is the corresponding wave number in vacuum. And the three important parameters for SPhP:  $k_{\text{SPhP}} = (\epsilon_1 \epsilon_2 / (\epsilon_1 + \epsilon_2))^{1/2} k_0$  is the wave number scilicet the propagation constant  $\beta$  along  $z$  direction and  $\alpha_1 = (k_{\text{SPhP}}^2 - \epsilon_1 k_0^2)^{1/2}$  and  $\alpha_2 = (k_{\text{SPhP}}^2 - \epsilon_2 k_0^2)^{1/2}$  are the corresponding lateral attenuation factors in vacuum and ITPC, respectively. As shown in Fig. 3, it is clearly that the spoof SPhP lies in the forbidden gap of the bulk phonon polariton. This is caused by the different mechanisms of the bulk and surface polariton effects in an ITPC. The real part of  $k_{\text{SPhP}}$  increases until a maximum value in the frequency  $f_s$ , represented by red solid line. The imaginary of  $k_{\text{SPhP}}$  also increases until a maximum value, as shown by red dashed line.

In our calculation, we take frequency  $f_s = 529$  MHz, with wavelength  $\lambda = 0.5667$  m. The corresponding permittivity of ITPC can be calculated from Eq. (4)  $\epsilon_2 = -8.6500 + 8.5871i$ .<sup>19</sup> In this case, the wave number  $k_{\text{SPhP}} = 11.4085 + 0.3498i$   $\text{m}^{-1}$ , wherein the imaginary part represents the absorption. And related lateral attenuation factors are

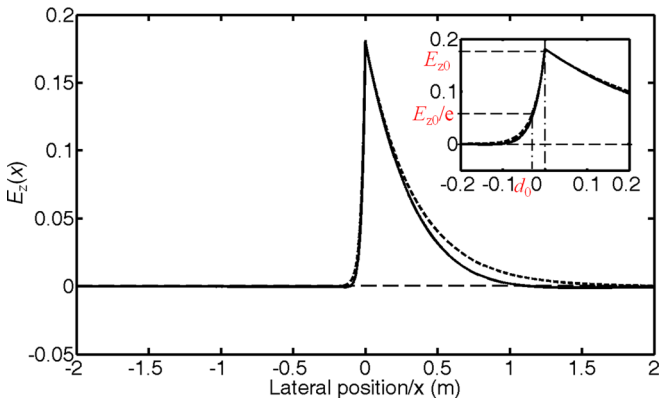


FIG. 4. The electric field ( $E_z$ ) distribution of SPhP mode, herein  $f_s = 529$  MHz with  $\alpha_1 = 2.9831 + 1.3377i$   $\text{m}^{-1}$  and  $\alpha_2 = 37.2906 - 14.0459i$   $\text{m}^{-1}$ . The interface of ITPC and vacuum is set at  $x = 0$ , left part represents ITPC and right part represents vacuum. The solid line represents real part of  $E_z$ , the dashed line represents absolute value of  $E_z$ . The illustration in the upper right corner depicts the  $E_z$  distribution near  $x = 0$  more clearly.

$\alpha_1 = 2.9831 + 1.3377i$   $\text{m}^{-1}$  and  $\alpha_2 = 37.2906 - 14.0459i$   $\text{m}^{-1}$ . Figure 4 shows that the EM field is confined at the interface of vacuum and ITPC. The EM field is strongest at the interface and attenuates to both sides in ITPC and vacuum simultaneously. In particular, the EM field attenuates very quickly in ITPC.  $d_0$  is defined to depict the EM field distribution normal to the interface where the EM field decay to  $1/e$ . Therefore, in the ITPC  $d_0 = 1/\text{Re}(\alpha_2) = 0.0268$  m. It is seen that  $d_0$  is far less than  $\lambda$ , and  $d_0 \approx 0.05\lambda$ . EM field is confined in a region much smaller than wavelength. That is to say, subwavelength optical phenomenon in microwave band is achieved by employing ITPC. As a consequence, we extend the frequency range of SPhP to microwave band which is impossible in natural ionic crystals.

At sufficiently low frequencies, dissipation must take charge. Since the imaginary part of  $k_{\text{SPhP}}$ , the EM energy will be attenuated when the spoof SPhP propagates forward. Figure 5 describes the change of EM field ( $E_z$ ) at the interface ( $x = 0$ ) when the spoof SPhP propagates forward along  $z$  direction. Generally, the EM energy is proportional to the square modulus of  $E_z$ . Thus, it is clear that the EM field is keeping attenuation with propagation forward. That is to say, there is an effective propagation length ( $l_0$ ) for this spoof SPhP.  $l_0$  is defined where the EM field decay to  $1/e$ . In our simulation,  $k_{\text{SPhP}} = 11.4085 + 0.3498i$   $\text{m}^{-1}$ , wherein the imaginary part is  $\kappa = \text{Im}(k_{\text{SPhP}}) = 0.3498$   $\text{m}^{-1}$  which determines the decay ratio of EM field. According to the definition of  $l_0$ , it is straightforward that  $l_0 = 1/\kappa = 2.8588$  m,  $l_0$  is larger than  $\lambda$ ,  $l_0 \approx 5.0\lambda$ . That is to say, the spoof SPhP can propagate a certain distance at the interface of ITPC and vacuum although  $l_0$  is not long enough. This is significant in practical applications.

In order to extend the propagation length, we should know that the vacuum is lossless and dissipation is resulted by imaginary part of ITPC dielectric permittivity. According to Eq. (6), we get the imaginary part

$$\text{Im}(\epsilon) \approx \gamma \omega \epsilon(\infty) \frac{\omega_{LO}^2 - \omega_{TO}^2}{(\omega^2 - \omega_{TO}^2)^2}. \quad (8)$$

That is to say, if the materials chose in ITPC has a smaller damping factor  $\gamma$ , the imaginary part of dielectric

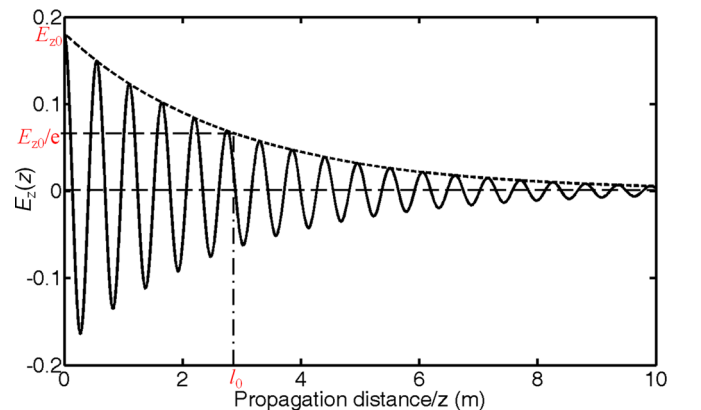


FIG. 5. The propagation of SPhP, herein  $f_s = 529$  MHz with  $k_{\text{SPhP}} = 11.4085 + 0.3498i$   $\text{m}^{-1}$ . The solid line represents real part of  $E_z$ , the dashed line represents absolute value of  $E_z$ .

permittivity  $\varepsilon$  of ITPC is decreased. Usually,  $\omega_s \sim \omega_{LO}$ , Eq. (8) can be further modified

$$\text{Im}(\varepsilon(\omega_s)) \approx \frac{\gamma\omega_s\varepsilon(\infty)}{\omega_{LO}^2 - \omega_{TO}^2}. \quad (9)$$

With larger difference between  $\omega_{LO}$  and  $\omega_{TO}$ , the imaginary part of dielectric permittivity  $\varepsilon(\omega_s)$  of ITPC is decreased. Therefore, the imaginary part of  $k_{SPhP}$ , namely  $\kappa$ , caused by the material dissipation will reduce via smaller damping factor  $\gamma$  or larger angular eigenfrequency squared difference  $\omega_{LO}^2 - \omega_{TO}^2$ . The propagation distance  $l_0$  is extended.

In an actual case, the PPLN has the typical thickness around 0.5–1 mm which is smaller than  $d_0$ . In this case, the sample has a sandwich structure. A thin layer of ITPC is covered by both sides of normal dielectric cladding with low loss, e.g., air or glass. The EM field will penetrate more into the cladding. Assume that there is no loss in the cladding media, the propagation distance  $l_0$  of spoof SPhP would increase remarkably, similarly to the long range surface plasmon polariton (LRSPP) waveguide.<sup>24</sup>

In this work, we only considered a simple ITPC with 1D periodicity. However, the modulation of ITPC could have different types and structures, which even may be extended to quasiperiodic, aperiodic, or two-dimensional (2D) superlattice.<sup>20</sup> In addition, since the SPhP gives rise to many subwavelength photonic devices, various subwavelength microwave device are also expected based on spoof SPhP effects in ITPCs. Borrowing the mature 1D/2D domain engineering in LiNbO<sub>3</sub>, we believe the PPLN based SPhP device will play an important role in future acoustic and microwave applications.

In conclusion, the ITPC that is comprised of two kinds or two domains of piezoelectric media is equivalent to a scale enlarged ionic crystal. Just like normal ionic crystals, polaritons could be excited due to the coupling between EM field and lattice or superlattice vibration. In comparison with the previously reported bulk polariton, our current findings in this work predict a spoof SPhP mode. Both fundamental mechanism, such as the dispersion relation, and technical applications exhibit some differences. For example, the frequency of the generated spoof SPhP is right at the forbidden band gap of bulk polariton with negative permittivity, as shown in Figs. 2 and 3. Since the structure and period of an ITPC could be designed and fabricated freely, the corresponding polariton frequency region thus is adjustable. Inter-

esting EM effects such as spoof SPhP in the megahertz region is predicted, which gives opportunities to control radiation at surfaces over a wide spectral range. In addition, the EM field enhancement associate with the spoof SPhP further results in many promising applications in microwave frequencies, such as subwavelength scale waveguide, EM sensing and detection, signal processing, and even some nonlinear devices.

This work is supported by 973 Programs under Contract No. 2011CBA00205 and 2012CB921803, and the PAPD, Fundamental Research Funds for the Central Universities. Yan-qing Lu appreciates the support from National Science Fund for Distinguished Young Scholars.

<sup>1</sup>G. Borstel and H. J. Falge, *Appl. Phys.* **16**, 211 (1978).

<sup>2</sup>D. K. Gramotnev and S. I. Bozhevolnyi, *Nat. Photonics* **4**, 83 (2010).

<sup>3</sup>E. Ozbay, *Science* **311**, 189 (2006).

<sup>4</sup>W. L. Barnes, A. Dereux, and T. W. Ebbesen, *Nature (London)* **424**, 824 (2003).

<sup>5</sup>S. H. Kwon, J. H. Kang, S. K. Kim, and H. G. Park, *IEEE J. Quantum Electron.* **47**, 1346 (2011).

<sup>6</sup>T. Holmgaard and S. I. Bozhevolnyi, *Phys. Rev. B* **75**, 245405 (2007).

<sup>7</sup>Z. Fei, A. S. Rodin, G. O. Andreev, W. Bao, A. S. McLeod, M. Wagner, L. M. Zhang, Z. Zhao, M. Thiemens, G. Dominguez, M. M. Fogler, A. H. Castro Neto, C. N. Lau, F. Keilmann, and D. N. Basov, *Nature (London)* **487**, 82 (2012).

<sup>8</sup>A. Huber, N. Ocelic, D. Kazantsev, and R. Hillenbrand, *Appl. Phys. Lett.* **87**, 081103 (2005).

<sup>9</sup>K. Torii, T. Koga, T. Sota, T. Azuhata, S. F. Chichibu, and S. Nakamura, *J. Phys.: Condens. Matter* **12**, 7041 (2000).

<sup>10</sup>A. Mohamed, G. E. Aitzol, S. Martin, H. Rainer, and A. Javier, *Chin. Sci. Bull.* **55**, 2625 (2010).

<sup>11</sup>S. Shen, A. Narayanaswamy, and G. Chen, *Nano Lett.* **9**, 2909 (2009).

<sup>12</sup>N. Ocelic and R. Hillenbrand, *Nat. Mater.* **3**, 606 (2004).

<sup>13</sup>J. J. Greffet, R. Carminati, K. Joulain, J. P. Mulet, S. Mainguy, and Y. Chen, *Nature (London)* **416**, 61 (2002).

<sup>14</sup>T. Taubner, F. Keilmann, and R. Hillenbrand, *Nano Lett.* **4**, 1669 (2004).

<sup>15</sup>G. Shvets, *Phys. Rev. B* **67**, 035109 (2003).

<sup>16</sup>J. B. Pendry, A. J. Holden, W. J. Stewart, and I. Youngs, *Phys. Rev. Lett.* **76**, 4773 (1996).

<sup>17</sup>J. B. Pendry, L. Martin-Moreno, and F. J. Garcia-Vidal, *Science* **305**, 847 (2004).

<sup>18</sup>K. Huang, *Proc. R. Soc. London, A* **208**, 352 (1951).

<sup>19</sup>Y. Q. Lu, Y. Y. Zhu, Y. F. Chen, S. N. Zhu, N. B. Ming, and Y. J. Feng, *Science* **284**, 1822 (1999).

<sup>20</sup>Y. Y. Zhu, X. J. Zhang, Y. Q. Lu, Y. F. Chen, S. N. Zhu, and N. B. Ming, *Phys. Rev. Lett.* **90**, 053903 (2003).

<sup>21</sup>X. J. Zhang, R. Q. Zhu, J. Zhao, Y. F. Chen, and Y. Y. Zhu, *Phys. Rev. B* **69**, 085118 (2004).

<sup>22</sup>H. F. Tiersten, *J. Acoust. Soc. Am.* **70**, 1567 (1981).

<sup>23</sup>M. Hase and M. Kitajima, *J. Phys.: Condens. Matter* **22**, 073201 (2010).

<sup>24</sup>A. Boltasseva, T. Nikolajsen, K. Leosson, K. Kjaer, M. S. Larsen, and S. I. Bozhevolnyi, *J. Lightwave Technol.* **23**, 413 (2005).